Pixel-based time-intensity curve analysis and apparent diffusion coefficient mapping of sinonasal organized hematomas

Miho Sasaki and Takashi Nakamura

Department of Radiology and Cancer Biology
Nagasaki University School of Dentistry

Address correspondence to:
Takashi Nakamura, DDS, PhD
Professor and Chief
Department of Radiology and Cancer Biology
Nagasaki University School of Dentistry
1-7-1 Sakamoto, Nagasaki 852-8588, Japan
Tel: +81-95-819-7707
Fax: +81-95-819-7711
E-mail: taku@nagasaki-u.ac.jp

Abstract

We present dynamic contrast-enhanced (DCE) and diffusion-weighted (DW) MR imaging features in 3 cases of sinonasal organized hematoma. DCE MR images were evaluated by analysis of time-intensity curve (TIC) patterns on a pixel-by-pixel basis (MR factor analysis) and DW MR images by analysis of apparent diffusion coefficient (ADC) maps. Preoperative information on the physiological tumor properties obtained with these MR imaging techniques may be useful in differentiating between organized hematoma and other benign and malignant sinonasal tumors.

Key Words: Sinonasal organized hematoma; dynamic contrast-enhanced MR imaging; diffusion-weighted MR imaging; MR factor analysis; apparent diffusion coefficient

Introduction

A sinonasal organized hematoma is an uncommon nonneoplastic benign lesion that can be potentially aggressive and extend into the surrounding structures in the maxilla. Patients with sinonasal organized hematomas often present with frequent epistaxis, nasal congestion, and rhinorrhea, mimicking malignant lesions. Histopathologically, the organized hematoma is composed of fibrous tissues surrounding an organized or old hematoma.

CT and MR imaging features of sinonasal organized hematoma have been relatively well documented [1, 2]; the lesion is often described as an expansile soft tissue mass with sinus wall erosion, heterogeneous signal intensity with a hypointense peripheral rim on fat-suppressed T2-weighted MR images, and irregular nodular, or papillary enhancement after contrast medium injection. However, the imaging features are often nonspecific among benign and malignant sinonasal tumorsand tumor-like lesions. Here, we adopted time-intensity curve (TIC) analysis on pixel-by-pixel basis (MR factor analysis) and 2-dimentional (2D) apparent diffusion coefficient (ADC) measurement (ADC map analysis) for further characterization of sinonasal hematomas.

Case reports

Case 1

A 36-year-old man presented with a history of repeated epistaxis on the right side. MR imaging revealed a sinonasal mass with homogeneous signal intensity on T1-weighted MR images and mixed areas of high and intermediate signal intensities on fat-suppressed T2-weighted images (Fig. 1A, B). Dynamic contrast-enhanced (DCE) MR images exhibited ink-droplet areas of core enhancement and peripheral areas of poor enhancement (Fig. 1C). MR factor analysis demonstrated that the mass was almost entirely (93%) composed of nonenhanced or slowly enhanced tissues (Fig. 1D, Table 1). An ADC map of this sinonasal mass displayed that overall ADC level was intermediate, with 49% of areas having extra-low or low ADCs (Fig. 1E, Table 1).

The histological diagnosis was organizing hematoma, consisting of central areas of hematoma with organized areas in the periphery (Fig. 1F). Small areas of granulation tissues were also found.

Case 2

A 29-year-old man presented with epistaxis and nasal obstruction on the left side. T1-weighted and fat-suppressed T2-weighted images showed a sinonasal mass with heterogeneous signal intensities (Fig. 2A, B). The mass was heterogeneously enhanced with the enhanced tumor areas exhibiting lobular architecture (Fig. 2C), which roughly corresponded to the

high-intensity tumor area on the fat-suppressed T2-weighted images. MR factor analysis revealed that the tumor was composed of large areas (76%) of nonenhanced and slowly enhanced tissues on TIC patterns (Fig. 2D, Table 1). The ADC map showed that the overall ADC level was intermediate and over half the tumor had areas with extra-low or low ADCs (Fig. 2E, Table 1).

Histological examination revealed hematoma associated with fibrin, hemosiderin depositions, and infiltrating inflammatory cells (Fig. 2F); these features were consistent with organized hematoma.

Case 3

A 77-year-old woman had complained of repeated bleeding in the oral cavity for over 3 months. MR imaging demonstrated a mass lesion in the right maxillary sinus; the lesion was heterogeneous on both T1-weighted and fat-suppressed T2-weighted images, and it was irregularly enhanced after gadolinium injection (Fig. 3A – C). MR factor analysis revealed that the mass was mostly (95%) composed of tissues exhibiting nonenhanced or slowly enhanced TIC patterns (Fig. 3D, Table 1). A large region (73%) of the mass displayed extra-low or low ADCs on ADC maps (Fig. 3E, Table 1).

Histologically, the tumor was a partly organized hematoma associated with lamellar depositions of fibrin and red blood cells. Hemosiderin depositions were also observed (Fig. 3F).

Discussion

In this report, we described pixel-based TIC profiles and ADC distributions in 3 cases of sinonasal organized hematoma. The lesions exhibited dominant areas of nonenhanced (≤20% increment ratio) or slowly enhanced (<20% increment ratio plus >120 sec peak time) tumor areas on MR factor analysis, and the ADC maps of these organized hematomas displayed dominant areas of extremely-low (< 0.6×10^{-3} mm^2/s) or low (< 1.2×10^{-3} mm^2/s) areas of ADCs. These MR imaging features are consistent with the histological architectures of organized hematoma; the lesions usually consisted of 2 major histological components, the organized or nonorganized old hematoma areas, containing blood cells and fibrin depositions; and the fibrous tissues surrounding the hematoma, with occasional association of granulation tissues containing small amounts of cellular components. The nonenhanced areas (areas with flat TICs) may represent fibrosis, and the areas with slow TICs may represent bleeding. On the other hand, the areas with rapid-uptake TIC profiles may represent inflammatory or cell-rich components. The balance between these 3 distinctive components may greatly influence the MR imaging features of individual lesions.

Physiological properties of tumors can be estimated by a kinetic study after contrast-medium injection. The use of TICs is the most conventional method of assessing MR dynamic study. However, many tumors are composed of distinctive tissues having different TIC characteristics. Therefore, analyzing a large region of interest (ROI) in a histologically heterogeneous tumor may

result in spurious results with regard to tumor histology. To avoid this error, analyzing TICs on pixel-by-pixel basis may be a good idea. MR factor analysis was first introduced by Di Paola's group to characterize the contrast enhancement kinetics of head and neck tumors [3]. However, the resolution of the obtained images was insufficient for effective correlation between MR images and histology. More recently, Eida et al. applied this MR technique to salivary gland tumors using surface coils and successfully correlated the MR factor analysis images with tumor histology [4]. In the present report, we have applied this technique to deep lesions without significantly diminishing the image resolution. However, patient movement is still a major problem in the MR factor analysis.

Diffusion-weighted imaging has been employed in diagnosing extracranial lesions; for example, recent studies showed that ADC measurement was useful in differentiation between benign and malignant lesions of the lymph nodes and salivary glands [5, 6]. Low ADCs indicate limited diffusion of water molecules in the tissue. Theoretically, therefore, a tumor or a tumor area with low ADCs contains a greater numbers of cells than that with high ADCs. Consistent with this notion, the ADC map demonstrated that lymphomas and undifferentiated cancers had lower ADCs than well differentiated squamous cell carcinomas, and cell-rich areas had lower ADCs than matrix-dominant areas in benign salivary gland tumors [5, 6]. In organized hematomas, organized or coagulated hematoma areas may be associated with low ADCs. In the present 3 cases of organized hematoma, extra-low and low ADC areas composed

49–73% of the total tumor areas. The organized hematoma per se is not a cell-rich disease. Therefore, the variation in tumor areas with extra-low and low ADCs in these hematomas may reflect the proportion of organized and/or coagulated areas relative to the total tumor areas.

CT findings of sinonasal organized hematoma are rather nonspecific [7, 8]; the reported CT appearance of the disease included a large expansile mass with bony erosion of the maxillary sinus and heterogeneous high attenuation on contrast-enhanced CT. MR imaging of the disease has recently been systematically analyzed [1, 2]. However, the reported MR findings, too, are often nonspecific. Therefore, imaging information regarding tumor physiology obtained by dynamic contrast-enhanced MR imaging and diffusion-weighted imaging may be useful in differentiating this nonneoplastic benign lesion from other sinonasal tumor and tumor-like lesions.

In this report, we presented MR imaging features of sinonasal organized hematomas, placing emphasis on the TIC and ADC profiles of these tumor-like lesions. MR factor analysis and ADC mapping may provide preoperative tissue characterization of sinonasal tumors and tumor-like lesions.

References

1. Nishiguchi T, Nakamura A, Mochizuki K, Tokuhara Y, Yamane H, Inoue Y. Expansile organized maxillary sinus hematoma: MR and CT findings and review of literature. AJNR Am J Neuroradiol. 2007;28:1375-77.
2. Kim EY, Kim H-J, Chung S-K, Dhong H-J, Kim HY, Yim YJ, et al. Sinonasal organized hematoma: CT and MR imaging findings. AJNR Am J Neuroradiol. 2008;29:1204-08.
3. Zagdaniski AM, Sigal R, Bosq J, Bazin JP, Vanel D, Di Paola R. Factor analysis of medical image sequence in MR of head and neck tumors. AJNR Am J Neuroradiol. 1994;15:1359-68.
4. Eida S, Ohki M, Sumi M, Yamada T, Nakamura T. MR factor analysis: improved technology for the assessment of 2D dynamic structures of benign and malignant salivary gland tumors. J Magn Reson Imaging. 2008;27:1256-62.
5. Sumi M, Nakamura T. Diagnostic importance of focal defects in the apparent diffusion coefficient-based differentiation between lymphoma and squamous cell carcinoma nodes in the neck. Eur Radiol. 2009;19:975-81.
6. Eida S, Sumi M, Sakihama N, Takahashi H, Nakamura T. Apparent diffusion coefficient mapping of salivary gland tumors: prediction of the benignancy and malignancy. AJNR Am J Neuroradiol. 2007;28:116-21.
7. Lee HK, Smoker WR, Lee BJ, Kim SJ, Cho KJ. Organized hematoma of the maxillary sinus: CT findings. AJR Am J Roentgenol. 2007;188:W370-3.

8. Song HM, Jang YJ, Chung Y-S, Lee B-J. Organizing hematoma of the maxillary sinus. Otolaryngol Head Neck Surg. 2007;136:616-20.
9. Eida S, Sumi M, Nakamura T. Multiparametric MR imaging for the differentiation between benign and malignant salivary gland tumors. J Magn Reson Imaging. 2010;31:673-79.

Figure Legends

Figure 1

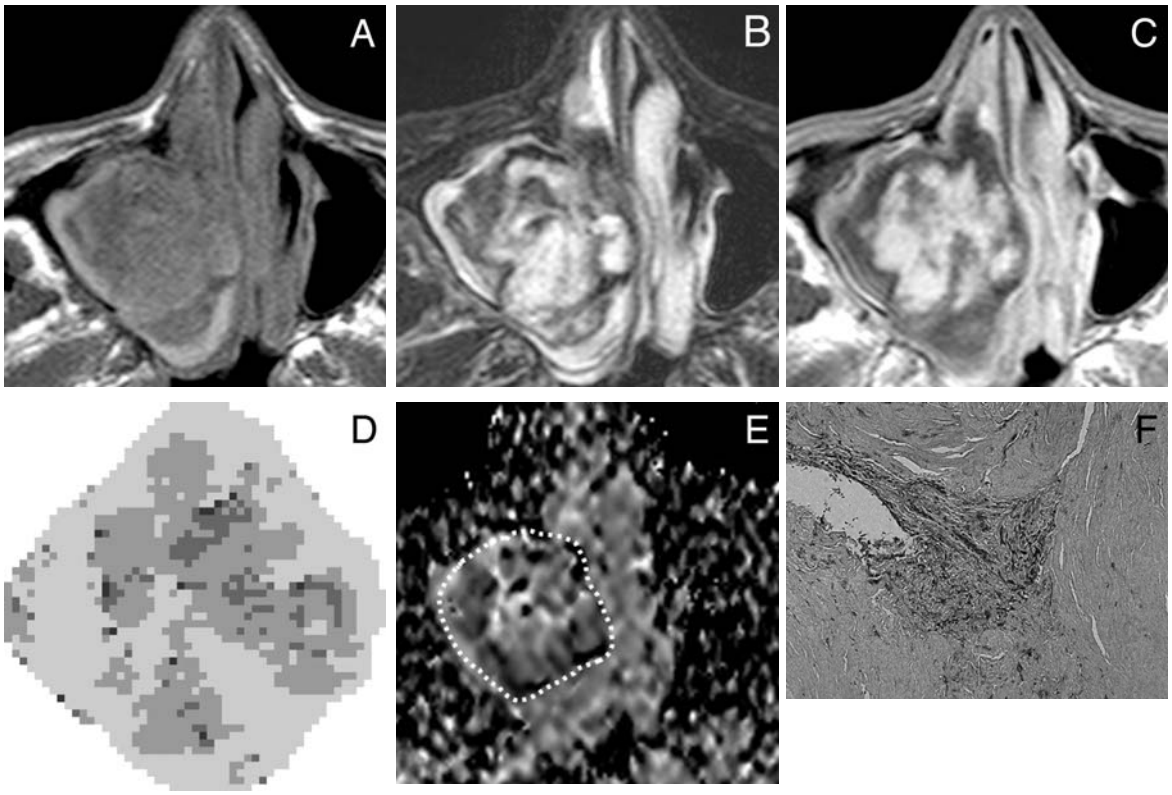

36-year-old man with sinonasal organized hematoma.

A, Axial T1-weighted MR image (TR/TE/number of signal acquisitions = 500 ms/15 ms/2) shows an expansile, homogeneous mass in the right maxillary sinus.

B, Axial fat-suppressed T2-weighted MR image (TR/TE/number of signal acquisitions = 6385 ms/80 ms/2) shows heterogeneous sinonasal mass.

C, Axial, contrast-enhanced T1-weighted MR image (TR/TE/number of signal acquisitions = 306 ms/10 ms/1) shows sinonasal mass with ink-droplets enhancement in the core; the tumor periphery is not enhanced (**D**).

D, MR factor analysis shows 2D distributions of tumor areas with type 1 (flat, light grey), type 2 (slow uptake, grey), type 3 (rapid uptake/low washout-ratio, dark grey), or type 4 (rapid uptake/high wash-out ratio, black) TIC profiles.
E, ADC map shows 2D distributions of tumor areas with extremely low (black), low (dark grey), intermediate (grey), or high (light grey) ADCs. Broken line indicates an ROI placed on the tumor area.
F, Photomicrograph shows fibrosis associated with small vessels and cell infiltrations. This histology corresponds to tumor areas with type 2 TIC patterns on MR factor analysis (**D**). H & E staining (original magnification at ×10).

Figure 2

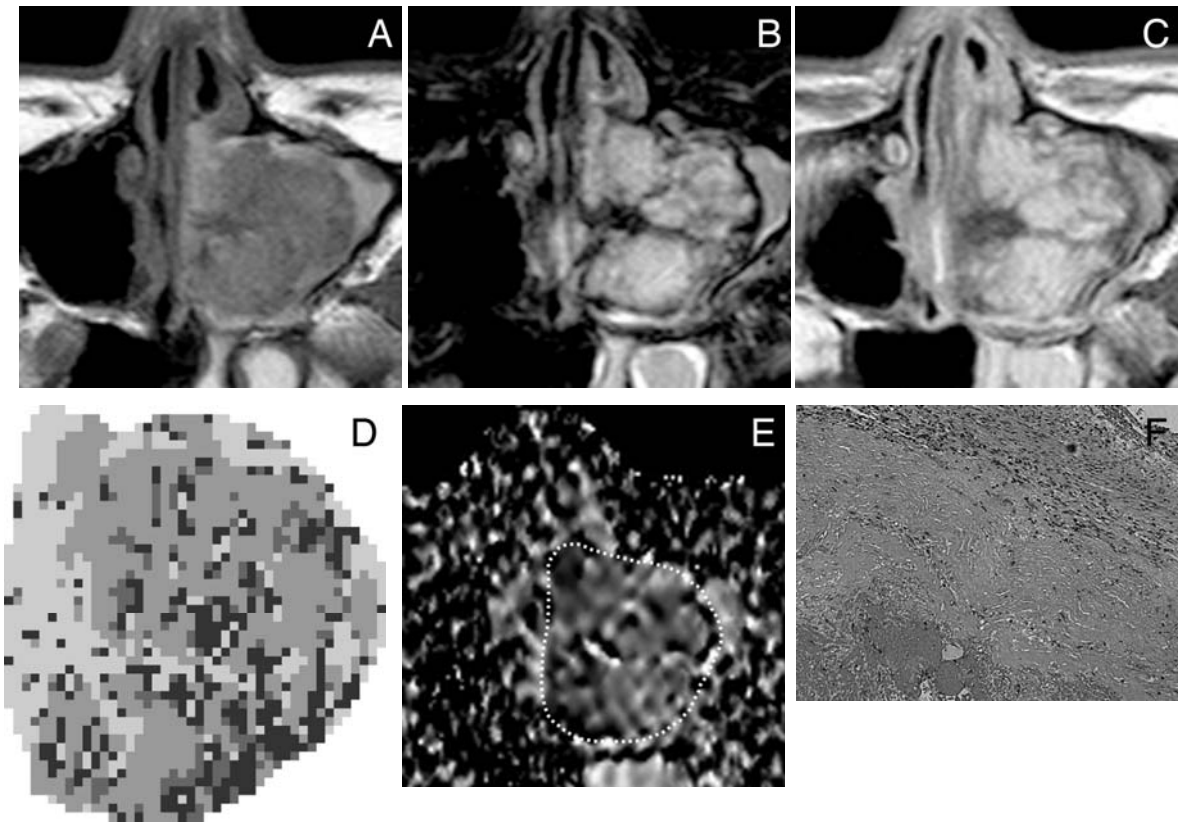

29-year-old man with sinonasal organized hematoma.

A, Axial T1-weighted MR image (TR/TE/number of signal acquisitions = 500 ms/15 ms/2) shows sinonasal mass with irregular signal intensity. Tumor intensity in the periphery is relatively high compared to its central part.

B, Axial fat-suppressed T2-weighted MR image (TR/TE/number of signal acquisitions = 6385 ms/80 ms/2) shows heterogeneous sinonasal mass.

C, Axial, contrast-enhanced T1-weighted MR image (TR/TE/number of signal acquisitions = 306 ms/10 ms/1) shows enhanced tumor areas in the inner part of the tumor.

D, MR factor analysis.

E, ADC map. Broken line indicates an ROI placed on a tumor area.

F, Photomicrograph shows fibrin deposition and old hematoma. Large areas of cell infiltration are also observed. This histology corresponds to tumor areas with type 1 or type 3/4 TIC profiles on MR factor analysis. H & E staining (original magnification at ×10).

Figure 3

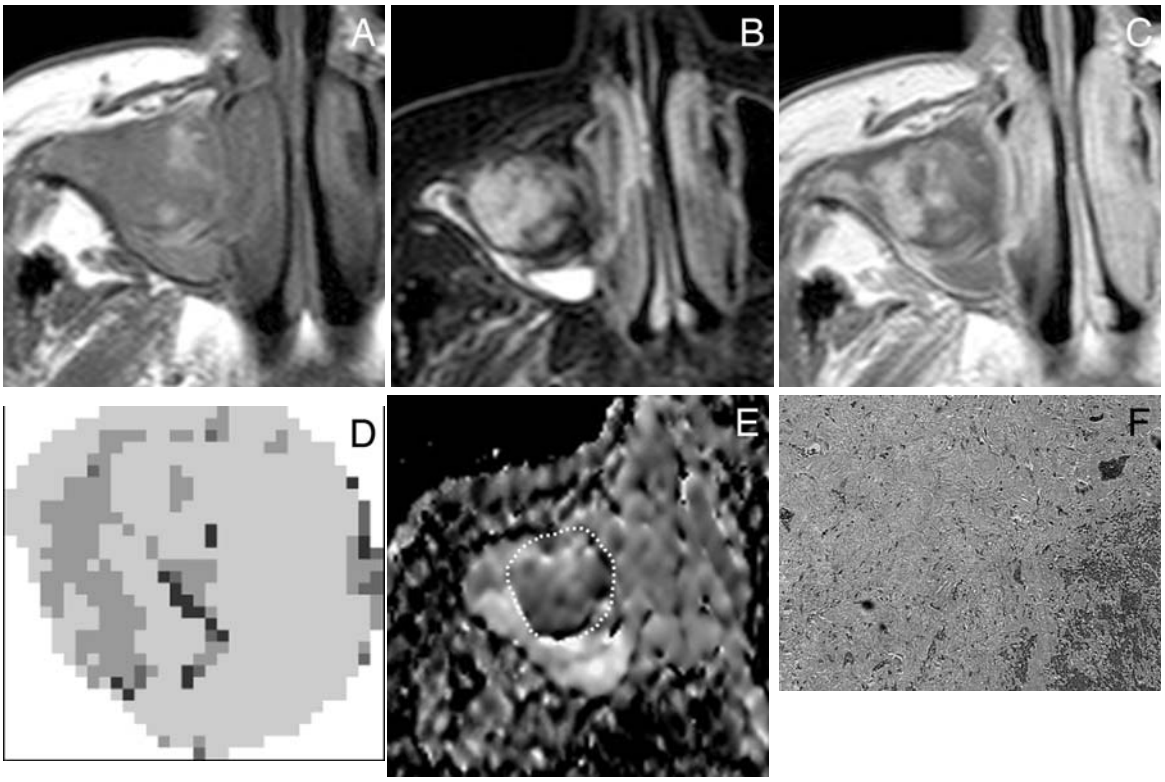

Fig. 3.—-77-year-old woman with organized hematoma.

A, Axial T1-weighted MR image (TR/TE/number of signal acquisitions = 500 ms/15 ms/2) shows sinonasal mass with irregular signal intensity.

B, Axial fat-suppressed T2-weighted MR image (TR/TE/number of signal acquisitions = 6385 ms/80 ms/2) shows heterogeneous sinonasal mass.

C, Axial, contrast-enhanced T1-weighted MR image (TR/TE/number of signal acquisitions = 306 ms/10 ms/1) shows irregular enhancement.

D, MR factor analysis.

E, ADC map. Broken line indicates an ROI placed on a tumor area.

F, Photomicrograph shows severe fibrin deposition with small areas of cell infiltration. Hemosiderin depositions are also

observed. This histology corresponds to tumor areas with type 1 TIC profiles on MR factor analysis. H & E staining (original magnification at ×10).

Table 1 Pixel-based TIC and ADC map

Case	Gender	Age	Overall ADC	Pixel-based TIC analysis (%)				ADC map (%)			
			($\times 10^{-3} mm^2/s$)	Type 1	Type 2	Type 3	Type 4	Extremely low	Low	Intermediate	High
1	M	36	1.2	60	33	6	1	13	36	40	12
2	M	29	1.1	27	49	10	14	22	37	27	14
3	F	77	0.9	72	23	4	2	22	51	23	4